Neuropsychopharmacology (2015) 40, 2753–2763

www.neuropsychopharmacology.org

Increased GABAergic Efficacy of Central Amygdala Projections to Neuropeptide S Neurons in the Brainstem During Fear Memory Retrieval

Kay Jüngling*[,1,3], Maren D Lange[1,3], Hanna J Szkudlarek[1,3], Jörg Lesting[1], Frank S Erdmann[1], Michael Doengi[1,4], Sebastian Kügler[2] and Hans-Christian Pape*[,1]

[1]Institute of Physiology I, Westfälische Wilhelms-Universität Münster, Münster, Germany; [2]Department of Neurology, Center for Nanoscale Microscopy and Molecular Physiology of the Brain (CNMPB), Universitätsmedizin Göttingen, Göttingen, Germany

The canonical view on the central amygdala has evolved from a simple output station towards a highly organized microcircuitry, in which types of GABAergic neurons in centrolateral (CeL) and centromedial (CeM) subnuclei regulate fear expression and generalization. How these specific neuronal populations are connected to extra-amygdaloid target regions remains largely unknown. Here we show in mice that a subpopulation of GABAergic CeL and CeM neurons projects monosynaptically to brainstem neurons expressing neuropeptide S (NPS). The CeL neurons are PKCδ-negative and are activated during conditioned fear. During fear memory retrieval, the efficacy of this GABAergic influence on NPS neurons is enhanced. Moreover, a large proportion of these neurons (~50%) contain prodynorphin and somatostatin, two neuropeptides inhibiting NPS neurons. We conclude that CeL and CeM neurons inhibit NPS neurons in the brainstem by GABA release and that efficacy of this connection is strengthened upon fear memory retrieval. Thereby, this pathway provides a possible feedback mechanism between amygdala and brainstem routes involved in fear and stress coping.
Neuropsychopharmacology (2015) **40,** 2753–2763; doi:10.1038/npp.2015.125; published online 20 May 2015

INTRODUCTION

The amygdala is a key region of the brain involved in processing and propagating fear- and anxiety-related signals. In recent years, much attention has been directed to the central amygdala (CeA), which is composed of the centrolateral (CeL) and centromedial (CeM) subnuclei. The prevalent view on the CeA as a mere output station of the amygdalar complex has been gradually replaced by a model in which highly organized synaptic circuits define functional entities related to specific components of fear processing. For instance, different subpopulations of CeL GABAergic neurons exist, which respond with increased or decreased activity to fearful stimuli ($fear_{on}$ or $fear_{off}$ neurons), and connect to CeM GABAergic neurons to gate fear expression and regulate fear generalization (Ciocchi *et al*, 2010; Haubensak *et al*, 2010; Tye *et al*, 2011; Li *et al*, 2013). Importantly, $fear_{on}$ or $fear_{off}$ neurons are characterized by the absence and presence of protein kinase C delta (PKCδ; Haubensak *et al*, 2010), and the majority of fear responsive neurons expresses the neuromodulatory peptide somatostatin (SOM; Li *et al*, 2013). Moreover, CeL neurons target neurons in the CeM, which in turn convey information to the brainstem (Ciocchi *et al*, 2010) and hypothalamus (Pare *et al*, 2004; Viviani *et al*, 2011). Activation of these pathways mediates behavioral fear and associated autonomic functions (Petrovich *et al*, 2001), although the identity of the brainstem target neurons and their upstream connectivity with the subpopulations of CeA neurons remain to be determined.

Within the brainstem, the locus coeruleus (LC) and the periLC region (Dimitrov *et al*, 2013; Reyes *et al*, 2011) are of particular interest, given their involvement in stress-mediated changes in fear and fear memory (Charney, 2003; Itoi and Sugimoto, 2010; Sara, 2009). One candidate neuronal population linking fear, stress, and arousal are neuropeptide S (NPS) expressing neurons located in the periLC region (Liu *et al*, 2011; Xu *et al*, 2004). NPS mediates an anxiolytic-like effect and facilitation of fear extinction (Donner *et al*, 2010; Jungling *et al*, 2008; Okamura *et al*, 2011; Reinscheid, 2008; Reinscheid *et al*, 2005; Xu *et al*, 2004), thereby buffering stress-related influences (Chauveau *et al*, 2012; Ebner *et al*, 2011; Petrella *et al*, 2011). Moreover, neuroanatomical data provide evidence that neurons in the LC and periLC region are targeted by neurons from the CeL that contain neuropeptides such as dynorphin A and the corticotropin-releasing factor (Dimitrov *et al*, 2013; Reyes *et al*, 2007, 2008, 2011).

*Correspondence: Dr K Jüngling or Professor H-C Pape, Institute of Physiology I, Westfälische Wilhelms-Universität Münster, Robert-Koch-Str. 27a, Münster D-48149, Germany. E-mail: Kay.Juengling@gmx.de or hans-christian.pape@ukmuenster.de
[3]These authors contributed equally to this work.
[4]Current address: Institute of Physiology II, Rheinische Friedrich-Wilhelms-University, Bonn, Germany
Received 19 January 2015; revised 16 April 2015; accepted 24 April 2015; accepted article preview online 4 May 2015

Therefore, we hypothesized that fear-relevant CeL neurons connect to NPS neurons, thereby providing the synaptic basis for functional interactions between two major systems that mediate stress influences on fear reactions. Our experimental strategy was to (i) identify the neuronal population in the CeL which project onto NPS neurons in the brainstem, (ii) assess the GABAergic nature and the co-existence of SOM and dynorphin in these pathways, (iii) pinpoint the influence of fear training on the efficacy of these synaptic connections, and (iv) characterize the effects of dynorphin and SOM on the target NPS neurons in the periLC. Our findings show that neurons of the CeL and CeM control the activity of the NPS system via increased GABA release during conditioned fear. Moreover, the presence of dynorphin and/or SOM in a subpopulation of CeL neurons projecting to periLC NPS neurons indicate a possible fine-tuned interplay between these neuropeptidergic systems that alter stress-mediated anxiety in opposite manner.

MATERIALS AND METHODS

Animals

NPS-EGFP mice (transgenic NPS-EGFP mouse line E16; (Liu *et al*, 2011)) were bred with C57Bl/6J mice, and offspring was genotyped by PCR as described previously (Liu *et al*, 2011). Furthermore, C57Bl/6J mice were used in subsets of experiments. Mice were kept in a temperature- (21°C) and humidity-controlled (50–60% relative humidity) animal facility with access to food and water *ad libitum* and a 12 : 12 h light-dark cycle with lights on at 0600 hours. All animal experiments were carried out in accordance with European regulations on animal experimentation (European Committee Council Directive 86/609/EEC; National Research Council of the National Academies) and protocols were approved by the local authorities (Bezirksregierung, Münster, AZ 50.0835.1.0, G 53/2005), and the 'Landesamt für Natur, Umwelt und Verbraucherschutz Nordrhein-Westfalen' (reference number: 8.87–51.05.20.10.218 and AZ 84–02.04.2012.A206).

Retrograde Tracing and Viral Transfection

For retrograde tracing, 200 nl of the retrograde tracer cholera toxin subunit B (CTB) conjugated with Alexa Fluor 594 diluted in sodium phosphate-buffered saline (PBS) to 0.7% (w/v) was stereotaxically injected unilaterally into the NPS-neuron cluster at the LC (for details see Supplementary Material and Methods). After one week, animals injected with CTB were perfused with PBS followed with 4% buffered PFA and brains were processed as described in the Immunohistochemistry section.

For local cell transfection, a virus solution (300 nl) that contained a recombinant adeno-associated virus of serotype 6 (rAAV-6; titer of 5×10^9 vector genomes/μl) carrying transgenes of enhanced yellow fluorescent protein (EYFP) and channelrhodopsin (ChR2; H134R variant) under control of the neuron-specific *human synapsin I* (hSynI) promoter or an rAAV expressing mCherry under the control of hSynI was used (rAAV-mCherry; kind gift from Beat Lutz, Mainz). The rAAV solution was stereotaxically injected bi or unilaterally into the CeL (for details see Supplementary Material and Methods). After a period of 6–8 weeks, animals injected with rAAV-ChRh2 solution were used for *ex vivo* examination as described in Electrophysiology and Immunohistochemistry section.

Fear Training and Behavioral Analysis

Transgenic NPS-EGFP mice or untreated C57Bl/6J mice injected with rAAV underwent fear conditioning as previously described (Laxmi *et al*, 2003; Sangha *et al*, 2012; Seidenbecher *et al*, 2003) and were subdivided into two groups (paired and unpaired; for details see Supplementary Material and Methods section). Freezing, an innate defensive behavior defined as complete immobility with the exception of respiratory movements, was taken as a behavioral measurement of fear (Fanselow, 1980). The freezing was scored blind to the treatment of the animal. Freezing time was calculated as the mean percentage that animal spent frozen through out all four CS^+ presentations (10s/CS^+) during retrieval. Forty-five minutes after fear memory retrieval the animals were perfused for immunohistochemistry. Naive mice were home-cage controls (HCCs) without any behavioral protocol. For *ex vivo* slice recordings, trained animals were decapitated 1.5 h after retrieval.

Electrophysiology and Optogenetic Techniques

Transgenic NPS-EGFP mice of either sex were anaesthetized with Forene (Isoflurane, 1-chloro-2,2,2-trifluoroethyl-difluoromethylether; 2.5% in O_2; Abbot GmbH, Germany) and decapitated. Horizontal slices (300 μm thick) containing the LC were prepared. Whole-cell patch-clamp recordings (in voltage- or current-clamp mode) were performed as described previously (Jungling *et al*, 2008). For details see Supplementary Material and Methods. Recordings were done blindly to the treatment of the animal.

NPS-EGFP neurons at the LC were detected by their somatic fluorescence using a 520 nm LED and a 535 nm YFP emission filter. Recordings were done in the voltage-clamp mode using a high-chloride intracellular solution at a holding-potential of −65 mV. ChR2-containing fibers were readily visible by their EYFP fluorescence. The aCSF contained DNQX, AP5, and CGP55845 to pharmacologically isolate $GABA_A$-receptor-mediated currents. GABAergic transmission was evoked with field of view illumination with a UHP-Mic-460 nm LED (Prizmatix, USA) applying brief (250 μs) light pulses at 30% of max. intensity (set as 100% stimulation intensity during input–output relationship experiments). Responses to the stimuli lacking the typical IPSC kinetic and with amplitudes smaller than two times the SD of the noise were considered as failures.

Drug Testing

To analyze the effects of SOM (Abbiotec, USA) and the κ-opioid receptor agonist dynorphin A (dynA, 1–10 porcine; Anaspec, USA), NPS-EGFP neurons were recorded in the current-clamp mode at resting membrane potentials. For details see Supplementary Material and Methods.

Immunohistochemistry

Immunohistochemistry was done according to standard protocols (for details see Supplementary Material and

Methods). NPS-EGFP or C57Bl/6J mice were deeply anesthetized by intraperitoneally injection of sodium pentobarbital (100 mg/kg) and transcardially perfused with 20 ml of ice-cold PBS (pH 7.4), followed by 4% paraformaldehyde in 0.1 M phosphate buffer (pH 7.4). Depending on the experimental design, 30 µm thick coronal or horizontal slices were stained with the following primary antibodies: guinea pig anti-prodynorphin (1 mg/ml, Neuromics), chicken anti-GFP (10 mg/ml, Abcam), rabbit anti-pCREB$_{S133}$ (1 mg/ml, Millipore), mouse anti-PKCδ (250 µg/ml, BD Biosciences), goat anti-SOM (200 µg/ml, SantaCruz) or mouse anti-mCherry (1 mg/ml, Biorbyt).

Stained slices were analyzed with a laser scanning confocal microscope (Nikon eC1 plus) using an Achromatic LWD 16×/0.8w objective (Nikon) or a 40× oil immersion objective (Plan Apochromat 40.0×/0.95/0.14 Correction Ring spring-loaded, CGC 0.11–0.23 mm; Nikon). Images of pCREB fluorescence following paired or unpaired training were acquired blindly to the treatment of the animals. For details on quantification see Supplementary Material and Methods.

Statistics

All data sets were tested for statistically significant outliers using the Grubb's test (significance level $P<0.05$). Within-group-comparisons were done by using student's *t*-test (significance level: $^{*}P<0.05$; $^{**}P<0.01$). To analyze differences between different groups, a one-way or two-way ANOVA, followed by Bonferroni *post hoc* test was used (significance level: $^{*}P<0.05$; $^{**}P<0.01$).

RESULTS

Prodynorphin-Positive CeL Neurons Project to the periLC Region Neurons Containing NPS

On the basis of anatomical studies, indicating that the periLC region in the brainstem of mice receives synaptic input from the CeA (Dimitrov *et al*, 2013; Reyes *et al*, 2008,2011), we hypothesized that NPS neurons in the periLC region are targeted by neurons located in the CeL. To test this hypothesis, an anterograde tracing study was performed in NPS-EGFP mice by local injection of rAAV-hSynI-mCherry into the CeL (Figure 1a). In two out of four animals, the CeL was accurately targeted and mCherry expression was visible in horizontal slice preparations *ex vivo* (Figure 1b). Within the periLC region, mCherry-tagged axonal structures were detected within the cluster of NPS neurons (Figure 1c). These data indicate that NPS neurons in the periLC region receive afferents from the central nucleus, ie the CeL region, of the amygdala, in accordance with previous findings (Dimitrov *et al*, 2013).

To identify the cell types projecting from the CeL to the NPS neurons within the periLC, the retrograde tracer cholera toxin subunit B-Alexa Fluor 594 (CTB; 200 nl) was injected unilaterally to the brainstem of transgenic NPS-EGFP mice (Figure 2a). In 4/11 animals, the injection was centered within the cluster of NPS-EGFP neurons of the periLC with very limited spreading of the tracer into the surrounding tissue. An example of a representative CTB injection site is depicted in Figure 2a. To further specify the pathway of CeL

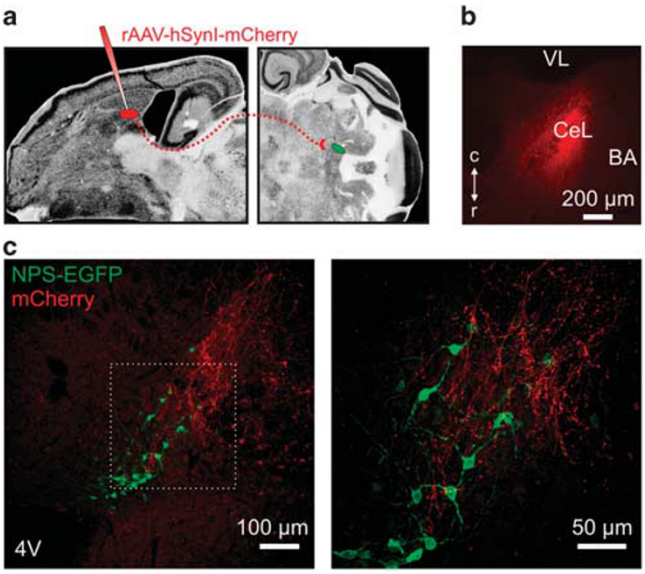

Figure 1 CeL neurons project to NPS neurons in the periLC region. (a) Scheme of rAAV-hSynI-mCherry injection into the CeL for anterograde tracing (modified after: mbl.org) to detect axons in the periLC region originating from CeL neurons. (b) Example of an injection site in the CeL in a horizontal slice preparation. Infected neurons express mCherry (red; VL, lateral ventricle; c, caudal; r, rostral). (c) In transgene NPS-EGFP mice ($n=4$), mCherry-positive fibers are overlapping with the NPS neurons cluster of the periLC region (4V, fourth ventricle). The tracing indicates that among other neurons, NPS neurons might be targeted by CeL neurons.

to NPS-neuronal connections, coronal slices containing retrogradely traced neurons within the CeA were identified and subjected to immunohistochemical stainings against PKCδ, prodynorphin (pdyn) and SOM. Examples of pdyn staining are depicted in Figure 2b. The mean number of pdyn-positive neurons was 41 ± 3 per slice calculated from 6 representative slices of each analyzed animal ($n=4$). In the CeL ipsilateral to the injection site, $59\pm3\%$ of the CTB-positive neurons were positive for pdyn (4 animals; Figure 2b and g), and $37\pm7\%$ of all detected pdyn-neurons were traced by CTB, whereas on the contralateral site no clear somatic CTB signals were detected. In addition, $54\pm4\%$ of CTB-positive neurons were positive for SOM ($n=4$; Figure 2e and g). In CTB-injected animals, no co-localization of CTB and PKCδ-positive neurons could be detected. In total, only $0.8\pm0.9\%$ of the CTB-positive neurons were co-localized with PKCδ (two animals; Figure 2c and g). Pdyn-positive neurons were located among PKCδ-positive neurons of the CeL, and the expression of the two proteins did not significantly overlap. Only $2.7\pm2.1\%$ of the pdyn-neurons were positive for PKCδ (three animals; Figure 2d and g), confirming previous findings (Haubensak *et al*, 2010). To test for a possible overlap of pdyn and SOM in the CeL, co-immunostainings were performed (Figure 2f and g). Indeed, a co-expression of pdyn and SOM was detected in $83\pm8\%$ (two animals) of all pdyn-neurons, indicating that the retrogradely labeled neurons represent a subgroup of the fear$_{on}$ neurons, being positive for pdyn and SOM. It should be noted that CTB-positive cells were regularly observed in the adjacent CeM (Figure 2b, d, and e), suggesting that CeM neurons also project to the periLC region. Overall, these data

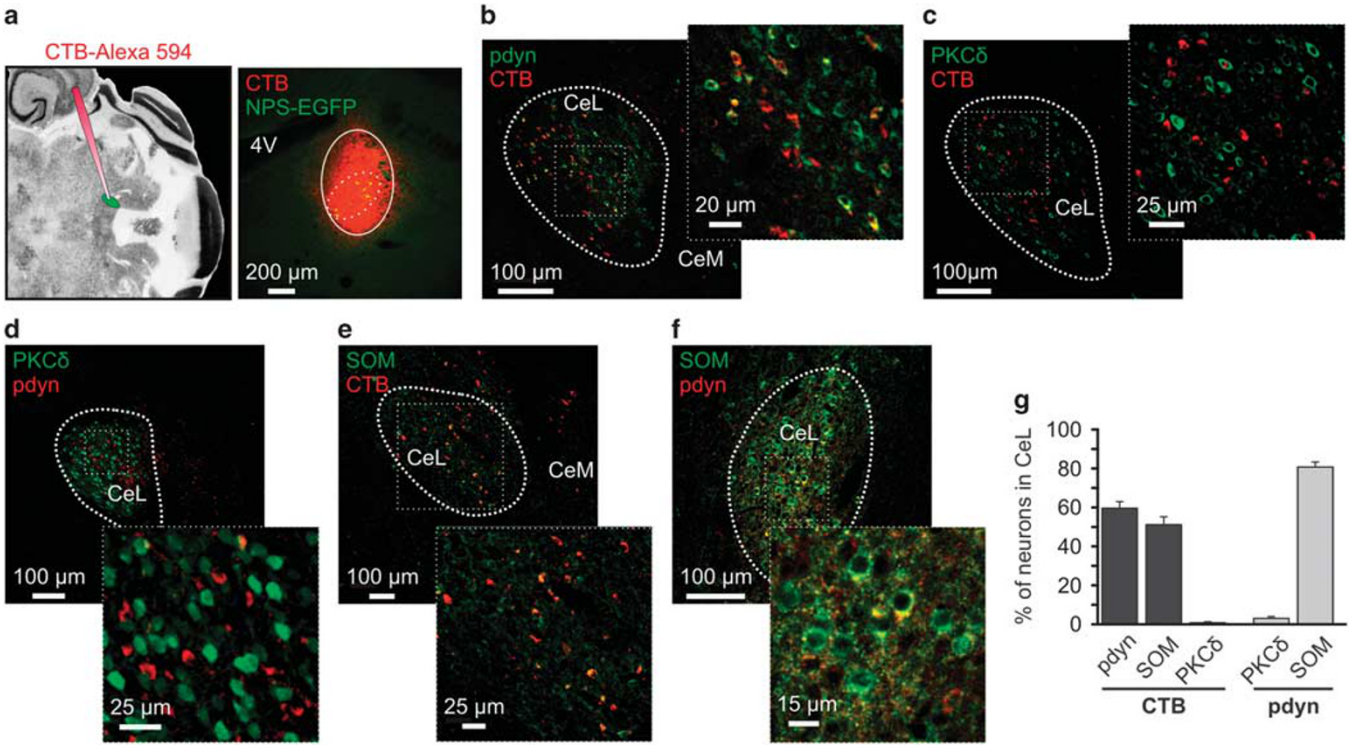

Figure 2 Retrogradely labeled neurons in the CeL are PKCδ-negative. (a) Scheme depicting the injection of the retrograde tracer CTB-Alexa594 into the periLC region (left panel; modified after: mbl.org). An example of a cholera toxin B-Alexa594 (CTB; red, right panel) unilateral injection in the NPS-EGFP cluster at the LC (4V: fourth ventricle). Solid circle marks the injection and the dashed circle outlines the location of the NPS-EGFP neurons within the slice. (b) Immunohistochemical stainings from CTB-injected animals against pdyn reveals co-localization of retrogradely transported CTB and pdyn within CeL neurons. (c) Immunohistochemical stainings from CTB-injected animals against PKCδ reveals no co-localization of retrogradely transported CTB and PKCδ within CeL neurons (d) Immunohistochemical staining against PKCδ (green) and pdyn (red) in coronal slices containing the CeL revealing that these peptides are expressed separately. (e) Immunostaining against SOM in the CeL of CTB-injected mouse. (f) Co-immunostaining against pdyn (red) and SOM (green) in the CeL. There was about two times more SOM- than pdyn-positive neurons detected. The vast majority (>80%) of pdyn-neurons was positive for SOM ($n=3$). (g) Percentage of CeL neurons that were CTB and pdyn-positive ($n=4$), CTB and SOM-positive ($n=4$), CTB and PKCδ-positive ($n=2$), pdyn- and PKCδ-positive ($n=3$), and pdyn- and SOM-positive ($n=2$).

indicate that neurons of the CeL and CeM project to NPS-EGFP neurons at the LC and that the CeL neurons are PKC*δ*-negative and express both SOM and pdyn.

Increased pCREB Expression in Dynorphinergic CeL Neurons after Fear Conditioning

It was shown that PKC*δ*-negative neurons are active during expression of fear (Haubensak *et al*, 2010; Li *et al*, 2013). Therefore we assessed the neuronal activation level in the CeL through detection and quantification of phosphorylated (serine 133) cAMP response element-binding protein (pCREB). CREB expression is increased during neuronal activity (Han *et al*, 2007; Hsiang *et al*, 2014; Izumi *et al*, 2011), and phosphorylation enhances activity of this transcription factor (Douglass *et al*, 1994). Two groups of mice (with paired and explicitly unpaired fear training) were subjected to immunohistochemical stainings against pCREB 45 min after fear retrieval (Figure 3a), and untreated mice were used as HCC to asses the basal levels of pCREB. Fear conditioning success was analyzed by measuring freezing during retrieval (Figure 3b). The paired group ($n=8$) showed $52.1\pm6\%$ freezing, which was significantly different from the unpaired group ($n=7$) with $11.9\pm5.31.7\%$ freezing upon CS^+ presentation, whereas in both groups freezing to the CS^- was low (paired CS^-: $17.3\pm5.4\%$; unpaired CS^-: $9.6\pm4.2\%$; one-way ANOVA: $F(3,26)=14.18$; $P=0.00001$; *post hoc* test: paired CS^+ *vs* paired CS^-: $P=1.5596E-4$; paired CS^+ *vs* unpaired CS^+: $P=2.6536E-4$).

Within the CeL, pCREB-positive nuclei were detected (Figure 3c) and analyzed in HCC, paired and unpaired groups (Figure 3c and d). In each individual mouse, the mean number of pCREB-nuclei per 10 000 µm^2 was calculated and normalized to the respective HCC. The mean absolute number of pCREB-positive nuclei in HCC was 6.6 ± 1.4 per 10 000 µm^2 ($n=9$). The number of pCREB-positive neurons was increased to $218\pm38\%$ of the HCC in the paired group ($n=8$) and to $102\pm23\%$ of the HCC in the unpaired group ($n=7$; Figure 3d). The increase observed in the paired group was significant (one-way ANVOA: $F(2,20)=5.58$; $P=0.003$; *post hoc* test: paired *vs* HCC: $P=0.0106$; paired *vs* unpaired: $P=0.029$; HCC *vs* unpaired: $P=0.903$).

These data show that upon fear memory retrieval in the paired group, a subpopulation of CeL neurons is activated as indicated by enhanced CREB phosphorylation. To address the question whether putative periLC-projecting neurons of the CeL expressing pdyn/SOM are activated during fear memory retrieval, the pCREB fluorescence intensity was measured in identified pdyn-positive neurons within the CeL

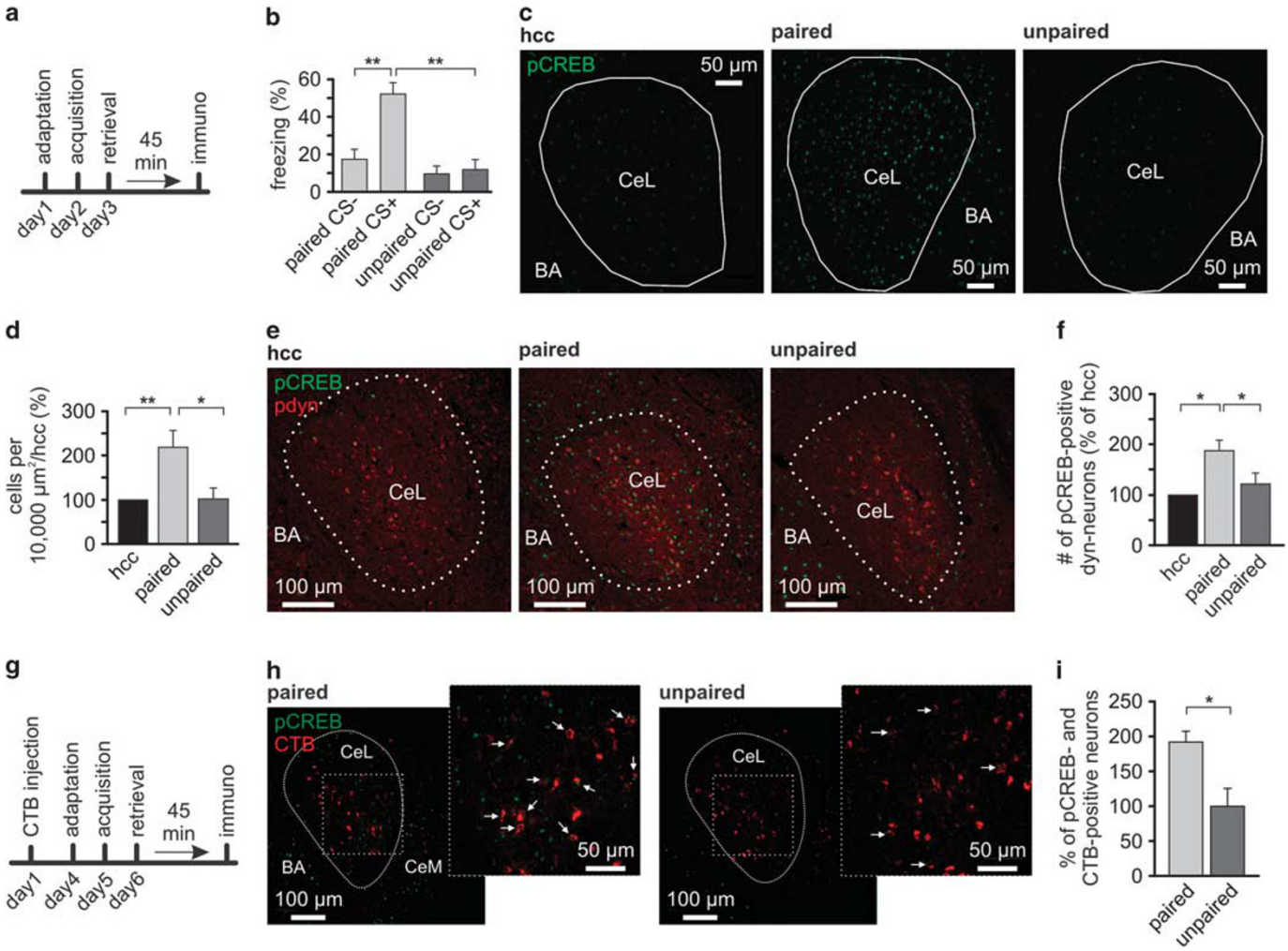

Figure 3 Expression of pCREB in dynorphinergic CeL neurons. (a) Scheme of the experimental design. (b) Quantification of freezing responses during retrieval in paired and unpaired groups. (c) Examples of immunohistochemical staining against pCREB(S133; green) in the CeL of home-cage controls (HCC) and after fear retrieval of paired and unpaired groups. (d) Quantification of pCREB-positive nuclei of the CeL neurons in the HCC ($n=9$ animals), paired ($n=8$ animals), and unpaired group ($n=7$ animals). After counting pCREB-positive nuclei per 10 000 μm^2 of the CeL, data were normalized to the HCC of each individual set. (e) Examples of co-staining for pdyn and pCREB(S133) in CeL of the HCC ($n=9$), paired ($n=8$), and unpaired ($n=7$) group. (f) Quantification of the normalized pCREB-positive nuclei in pdyn-positive neurons, normalized to the HCC of each individual set. (g) Scheme of experimental design. (h) Examples of immunohistochemical staining against pCREB (S133; green) in the CeL of CTB-injected mice after fear retrieval of the paired ($n=6$ animals) and unpaired ($n=6$ animals) groups. CTB was injected into the LC/periLC region and CTB-positive neurons (red) were detectable in the CeL. Note also the presence of some CTB-positive neurons in the CeM. (i) Quantification of the normalized percentage of pCREB-positive nuclei in CTB-positive neurons, normalized to the unpaired group of each individual set.

(Figure 3e). Analyzed samples were taken from the trained groups described above. The percentage of pdyn-positive neurons within the CeL that contained also pCREB was $35 \pm 3\%$ ($n=9$ animals) in HCC. Compared with HCC, the number of pCREB immunopositive pdyn-neurons increased to $187 \pm 21\%$ in the paired group, ($n=8$ animals), and to $121 \pm 22\%$ ($n=7$ animals) in unpaired mice. The increase of the percentage of pdyn-pCREB-positive nuclei in the paired group was significantly different from HCC or unpaired group (one-way ANOVA: $F(2,21)=8.19$; *post hoc* test: $P=4.3191E-4$ paired *vs* HCC; $P=0.046$ paired *vs* unpaired; Figure 3f). These data indicate that treating mice with foot shock increases pCREB intensities in pdyn-neurons compared with HCC, but paired CS^+/US conditioning significantly increases pCREB compared with pseudo-trained unpaired mice. In a next set of experiments mice received local, unilateral CTB-Alexa 594 injection into the LC/periLC region 3–4 days prior to paired or unpaired fear training (Figure 3g). The freezing was significantly increased in the paired ($n=6$) compared with the unpaired ($n=6$) group (paired CS^+: $38.2 \pm 4.2\%$; paired CS^-: $4 \pm 1.2\%$; unpaired CS^+: $2.9 \pm 0.9\%$; unpaired CS^-: $1.1 \pm 0.3\%$; one-way ANOVA: $F(3,20)=62.81$; $P=0.0001$; *post hoc* test: paired CS^+ *vs* paired CS^-: $P=4.54457E-4$; paired CS^+ *vs* unpaired CS^+: $P=9.85009E-6$). As described above, the pCREB expression was analyzed in CTB-positive nuclei of the CeL of paired and unpaired trained mice (Figure 3h). To minimize variations between different sets of experiments the data were normalized to the mean percentage of CTB- and pCREB-positive nuclei in the CeL of the unpaired group (Figure 3i). The

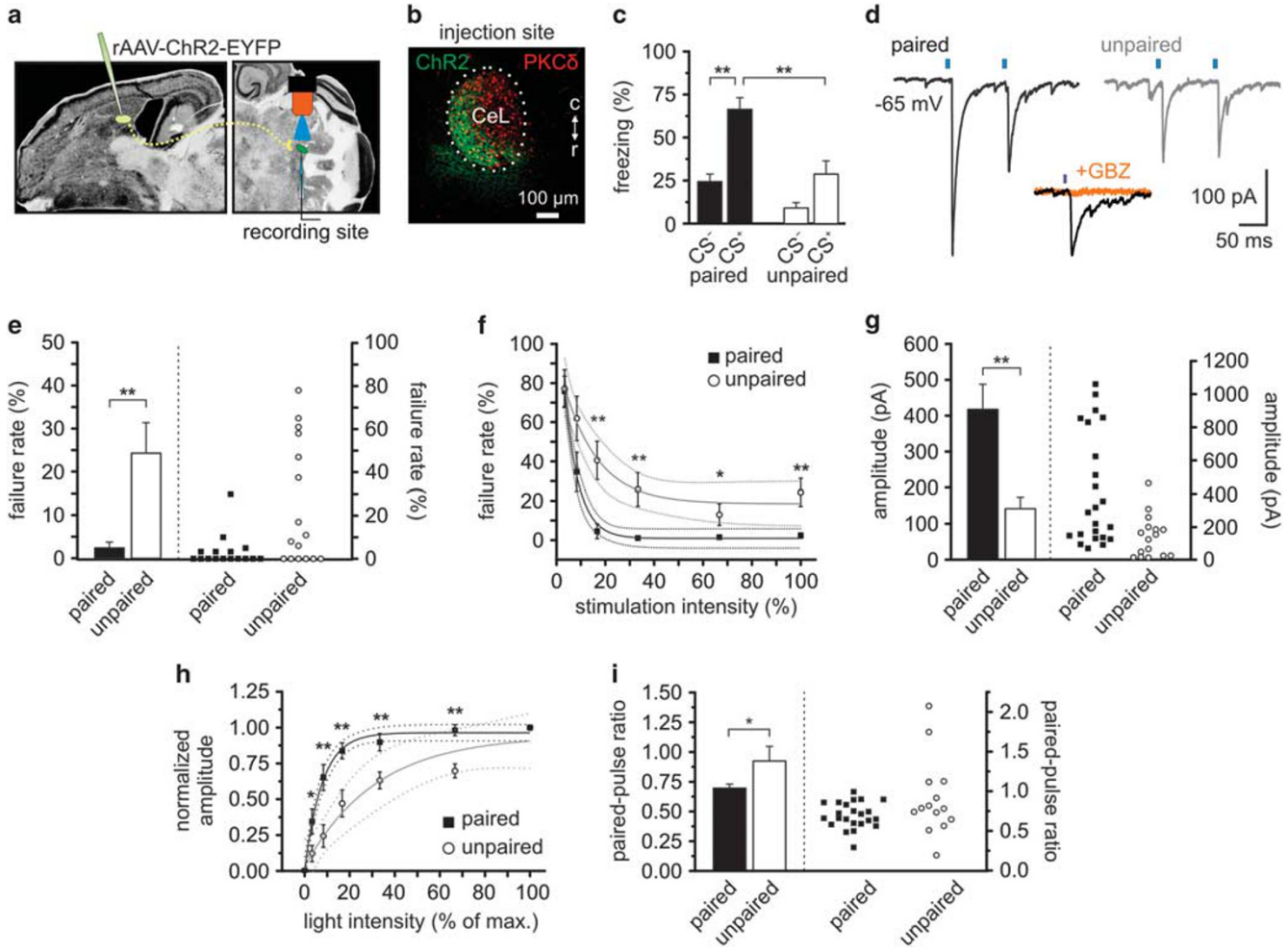

Figure 4 CeL neurons form GABAergic synapses on NPS neurons in the periLC region. (a) Scheme of the experimental design. rAAV solution was injected into the CeL and NPS-EGFP neurons in the periLC were recorded in horizontal slice preparations. GABA release was triggered by brief blue-light exposure (modified after: mbl.org). Example of an injection site (b) example of a horizontal slice with the injection site (ChR2-EYFP fluorescence) within the cluster of PKCδ-positive neurons of the CeL. (c) Quantification of freezing responses during retrieval in paired and unpaired groups of transgenic NPS-EGFP mice used for *ex vivo* recordings. (d) Examples of light-evoked GABAergic responses in the voltage-clamp mode in NPS neurons of paired and unpaired trained animals 1.5 h after fear retrieval. Light-evoked responses were sensitive to gabazine (GBZ; middle). (e) Quantification of the light-evoked IPSC failure rate recorded in paired ($n=23$ neurons/6 animals) and unpaired ($n=16$ neurons/4 animals) trained mice using maximal stimulation intensity. (f) Quantification of the failure rates at decreasing stimulation intensities recorded in the paired and unpaired mice. The data were fitted with an asymptotic function (solid lines) and the confidence intervals of the fit (95%) are depicted by the dashed lines. (g) Quantification of the mean success amplitude during maximal stimulation. (h) Input–output relationship (normalized IPSC amplitude *vs* relative light intensity) for paired ($n=15$ neurons/4 animals) and unpaired ($n=13$ neurons/4 animals) trained mice. The data were fitted with an asymptotic function (solid lines) and the confidence intervals of the fit (95%) are depicted by the dashed lines. (i) Quantification of the paired-pulse ratio (100 ms interval) of light-evoked IPSCs at maximal stimulation.

occurrence of pCREB-positive nuclei in CTB-positive CeL neurons was significantly increased in the paired ($n=6$ animals) group compared with unpaired trained mice ($n=6$ animals; one-way ANOVA: $F(1,10)=9.477$; $P=0.012$; Figure 3i). These data provide further evidence that LC/periLC-projecting CeL neurons are activated during fear memory retrieval following a paired training paradigm.

Fear Memory Retrieval Modulates GABAergic Synaptic Efficacy on NPS Neurons

As the retrograde tracer experiments provide only little information about functionality of synaptic connections, we used optogenetic approaches to functionally assess a monosynaptic connection between CeL neurons and NPS-EGFP neurons. A recombinant rAAV-6 coding ChR2 and EYFP under control of a hSynI promoter was injected into the CeL (Figure 4a and b). After 6–8 weeks, horizontal slices containing either the LC or the CeL were cut. Counterstaining of the CeL against PKC*δ* served as a criterion for the regional specificity of injection (Figure 4b). The injection sites of analyzed animals and examples of off-target injections are shown in Supplementary Figure 1. During voltage-clamp recordings from NPS-EGFP cells in the presence of DNQX, AP5, and CGP55845, at a holding-potential of −65 mV, brief light pulses (250 µs; 460 nm LED) evoked postsynaptic currents which were blocked by gabazine, and thus were believed to be GABAergic (Figure 4d). Of note,

only injections within or close to the CeL/CeM boundaries resulted in light-evoked responses in NPS neurons (Supplementary Figure 1A).

The above described increase of pCREB occurrence after fear memory retrieval indicates that exposure to fearful stimuli leads to neuronal activation. Therefore, in a next set of experiments, the possible influence of fear-related activity in CeL neurons on their functional synaptic connections to NPS neurons was tested. Six to eight weeks post rAAV-injection, mice were trained with the paired or unpaired paradigm, and 1.5 h after retrieval session horizontal slices were prepared to record neuronal activity *ex vivo*. The paired group ($n=6$) showed $66.3\pm6.7\%$ freezing, which was significantly different from the unpaired group ($n=4$) with $28.8\pm7.7\%$ freezing upon CS^+ presentation, whereas in both groups freezing to the CS^- was low (paired CS^-: $24.3\pm4.4\%$; unpaired CS^-: $9.1\pm3.1\%$; one-way ANOVA: $F(3,16)=17.95$; $P=0.00001$; *post hoc* test: paired CS^+ *vs* paired CS^-: $P=0.0004$; paired CS^+ *vs* unpaired CS^+: $P=0.0071$; Figure 4c).

In slices from all three groups of mice, $GABA_A$-receptor-mediated responses were elicited in NPS neurons by blue-light stimulation of ChR2 terminals in the periLC region. In the paired group the mean latency was 3.5 ± 0.3 ms ($n=23$ neurons/6 animals) and 3.6 ± 0.4 ms in the unpaired group ($n=16$ neurons/4 animals; unpaired *t*-test: $P=0.7758$). The SD of light-evoked IPSC onset latencies (jitter) was 0.3 ± 0.06 ms in the paired group and 0.28 ± 0.07 ms in the unpaired group (unpaired *t*-test: $P=0.859$). The apparent connectivity was estimated by dividing the number of recorded neurons with evoked response per animal by the total number of recorded neurons. The apparent connectivity was at $47\pm6.2\%$ (13 animals; with a minimum of 12.5% and a maximum of 80%), analyzed in mice from paired, unpaired, and HCC groups. Of note, the mean amplitudes of light-evoked IPSCs in each animal did not correlated with the fraction of infected CeL area ($Area_{YFP}/Area_{PKC\delta}$) as evident from the Pearson correlation ($r=-0.278$; $P=0.358$; Supplementary Figure 1B). In contrast, the apparent connectivity was positively correlated with the infected CeL area ($r=0.542$; $P=0.03$; Supplementary Figure 1C).

In order to assess the possible effects of behavioral training on functional GABAergic connections, the failure rates of IPSCs to the first stimulus, the success amplitude, and the paired-pulse ratio of IPSCs (two light stimuli at 30% of the maximal LED intensity; 100 ms interval) were analyzed (Figure 4d). The failure rate and the paired-pulse ratio are considered to be presynaptic parameters, depending on the release probability of the synapse, whereas the success amplitude is a factor influenced by both, pre- and postsynaptic parameters. The evoked responses in the paired group had a mean failure rate of $2.4\pm1.4\%$ ($n=23$ neurons/6 animals) and were significantly different from the failure rates of the unpaired group with $24.3\pm7.1\%$ ($n=16$ neurons/4 animals; one-way ANOVA: $F(1,37)=12.86$; $P=0.0009$; Figure 4e). The analysis of failure rates over all of used stimulation intensities revealed significant differences between paired and unpaired groups (two-way ANOVA with repeated measurements: training-based effect paired *vs* unpaired: $F(1166)=26.21$; $P=0.0001$; light intensity-based effect: $F(5,166)=31.02$; $P=0.0001$; but no significant interaction: $F(5,166)=1.54$; $P=0.18$; Figure 4f). The mean failure rates were significantly smaller in the paired group compared with the unpaired group at broad range of light intensities (paired *vs* unpaired at 100% of max. intensity: (unpaired *t*-test) $P=0.0031$ at 66%; $P=0.0313$ at 33%; $P=0.0036$ at 16%; $P=0.0008$ at 8%; $P=0.0806$ at 3%; and $P=0.9080$; Figure 4f).

The mean success amplitude was significantly increased in the paired group compared with the unpaired group (paired: 417.6 ± 70 pA and unpaired: 142.3 ± 31.6 pA; one-way ANOVA: $F(1,37)=9.73$; $P=0.0035$; Figure 4g). Of note, the mean success amplitude in paired animals was significantly larger than in HCC (190.8 ± 61 pA; $n=15$ neurons/3 animals) or unpaired, whereas HCC and unpaired were not significantly different (one-way ANOVA: $F(2,51)=6.21$; $P=0.0038$; *post hoc* test: paired *vs* HCC: $P=0.0295$; HCC *vs* unpaired: $P=0.48$).

The normalized amplitudes in the input–output curve (plotted normalized amplitudes *vs* relative light intensity) were significantly increased in the paired compared with the unpaired group (two-way ANOVA with repeated measurements: training-based effect paired *vs* unpaired: $F(1,26)=20.47$; $P=0.000109$; light intensity-based effect: $F(4,104)=38.67$; $P=0.00001E-13$; but no significant interaction: $F(4,104)=0.904$; $P=0.465$; $n=15$ neurons/4 animals paired; $n=13$ neurons/4 animals unpaired; Figure 4h). The normalized amplitudes recorded in paired and unpaired animals were significantly increased at all light intensities tested (paired *vs* unpaired at 66% of max. intensity: (unpaired *t*-test) $P=8.5283E-5$ at 33%; $P=0.0041$ at 16%; $P=0.0018$ at 8%; $P=0.0024$ at 3%; and $P=0.0472$; Figure 4h). The paired-pulse ratio of the evoked responses in the paired group was smaller compared with the unpaired group (paired: 0.7 ± 0.03; $n=23$ neurons/6 animals; unpaired: 0.92 ± 0.12; $n=15$ neurons/4 animals; one-way ANOVA: $F(1,36)=4.54$; $P=0.039$; Figure 4i). It should be noted that the difference in the paired-pulse ratio is mainly driven by a small fraction of recorded neurons, which limits the interpretation of this parameter. These findings indicate that fear conditioning reduces the failure rate and increases paired-pulse depression, suggesting increased release probability at GABAergic connections between CeL projection neurons and NPS-neuronal targets at the LC upon fear conditioning.

Because the data presented here indicate that CeL neurons projecting on NPS neurons in the periLC region might contain SOM and pdyn, the effect of these neuropeptides on NPS neurons was tested by exogenous application during current-clamp recordings. Immunohistochemical stainings confirmed the presence of both, pdyn and SOM, in fiber-like structures surrounding NPS neurons (Figure 5a). The application of 250 nM dynA induced a significant membrane hyperpolarization in all neurons tested ($n=12$ neurons/4 animals; Figure 5b and d). The mean membrane potential of NPS-EGFP neurons during baseline conditions was at -69.4 ± 1.2 mV and shifted to -79.5 ± 1 mV in the presence of dynA (ΔV: -11.5 ± 0.3 mV; $P=1.3567E-5$). To calculate changes of the input resistance during drug application, brief (500 ms) hyperpolarizing currents (−40 pA) were used. To analyze changes of the input resistance induced by the drug only and to minimize the impact of voltage-dependent conductances on the resistance, the membrane potential during maximal drug effect was set back to baseline values by

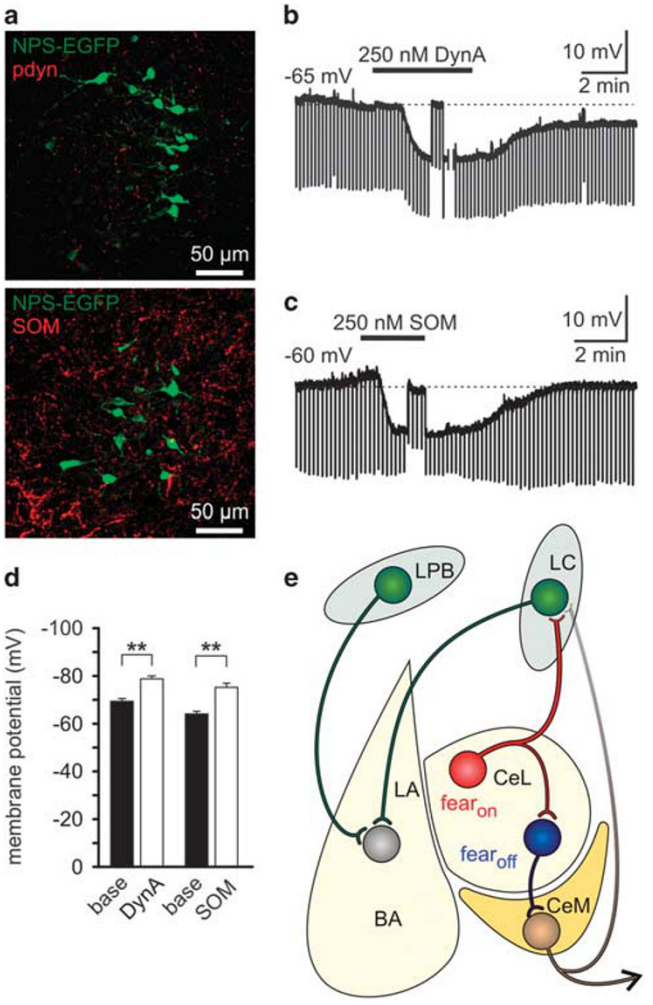

Figure 5 Dynorphin and somatostatin inhibit NPS neurons in the periLC region. (a) Immunostaining against pdyn and NPS-EGFP (top), and SOM and NPS-EGFP (bottom) in horizontal slice preparations. The stainings indicate the presence of both neuropeptides in the vicinity of NPS neurons in the periLC region. (b) Example of a current-clamp recording of the NPS neuron. Application of dynA hyperpolarizes the recorded neuron from a membrane potential of −65 mV. Hyperpolarizing current injections (−40 pA) were applied to analyze the input resistance. During maximal drug effect, the membrane potential was briefly manually clamped back to baseline values. A similar hyperpolarization was observed upon SOM-application at a membrane potential of −60 mV in a different NPS neuron (c and d) Quantification of the substance-induced changes of the membrane potential in NPS neurons. (e) Fear responsive (fear$_{on}$) neurons of the CeL inhibit via GABAergic synapses fear$_{off}$, PKCδ-positive CeL neurons, which form GABAergic synapses on the CeM output neurons. Activity of fear$_{on}$ neurons would disinhibit CeM neurons and thus allow eg freezing behavior (Ciocchi *et al*, 2010; Haubensak *et al*, 2010; Li *et al*, 2013). In addition, the CeL fear$_{on}$ neurons and CeM neurons form inhibitory GABAergic synapses on NPS neurons in the periLC region. LC and/or LPB (lateral parabrachial nucleus) NPS neurons in turn project to LA/BA of the amygdala and reduce anxiety or facilitate fear extinction via NPS-release. Terminals from the CeL and CeM release GABA onto NPS neurons and thus reduce their activity. A subset of CeL GABAergic inputs might contain, eg dynorphin and/or SOM, which could inactivate NPS neurons in the periLC when released.

manual voltage clamp. The mean input resistance was significantly decreased (baseline: 483 ± 22 MΩ; dynA: 348 ± 31 MΩ; $n = 11$ neurons/4 animals; $P = 0.0018$). Applications of 2.5 min or 5 min duration yielded similar responses.

Applying 250 nM SOM on NPS neurons at the LC during current-clamp recordings induced a hyperpolarization by −11.01 ± 2 mV, from −63 ± 1.1 mV to −74 ± 1.7 mV ($P = 8.5259E-4$; $n = 8/4$ animals; Figure 5c and d). In addition, the R_{in} of NPS neurons was reduced by 184 ± 40 MΩ compared with baseline ($P = 0.0026$; $n = 8$). To confirm that single NPS neurons are responsive for SOM and dynA, both agonists were applied subsequently in two individual recordings. In both recordings, the NPS neurons were hyperpolarized by SOM and dynA, indicating that receptors for both peptides are postsynaptically expressed by the same neurons. The hyperpolarizations, induced by single applications of either dynA or SOM, were not significantly different (one-way ANOVA: $F(1;18) = 0.63$; $P = 0.44$). These data provide evidence that SOM and dynA are suited to inhibit NPS-neuronal activity via activation of postsynaptic receptors.

DISCUSSION

It has been shown that central amygdalar projections to the brainstem are paramount for the expression of stress- and fear-related behaviors. The overriding aim of our study therefore has been to identify the synaptic connectivity between defined subpopulations of CeL neurons and their brainstem targets, to focus on transmitter systems involved in regulation of fear and stress responsiveness, and to assess the contribution of the synaptic interactions to conditioned fear. (i) We show here that among putative target neurons in the LC/periLC region a defined group of neurons, namely NPS neurons, is innervated by a subpopulation of CeL neurons, which can be classified as fear$_{on}$ neurons owing to the lack of PKCδ and expression of pdyn and SOM. (ii) In fact fear memory retrieval activates the neurons in the CeL, including the subpopulation of dynorphin and SOM expressing neurons, as indicated by increased levels of phosphorylated CREB. (iii) We provide direct evidence indicating that the connection between these CeL neurons and their NPS target neurons is of monosynaptic GABAergic nature, and that the efficacy of this connection is enhanced upon fear memory retrieval. (iv) Finally, we show that dynorphin and SOM exert an inhibitory influence on NPS neurons via stimulation of postsynaptic receptors.

Anatomical data in rodents (Dimitrov *et al*, 2013; Reyes *et al*, 2011; Figure 5e) have shown an abundance of connections between the CeL and the LC/periLC, but the identity of the target neurons and thereby the functional impact remained poorly understood. Optogenetic activation of ChR2-expressing CeL terminals in the present study proved the existence of monosynaptic, GABAergic connections from CeL and CeM neurons onto NPS neurons. Recording GABAergic transmission in the presence of specific glutamate receptor antagonists along with short and constant latencies of the monitored IPSCs rule out a gross indirect polysynaptic network contribution. It has been described earlier that the CeL neurons are responsive to fearful stimuli and contribute to information processing within the CeA (Haubensak *et al*, 2010). Moreover, excitatory synaptic influences from BA onto CeL neurons display plasticity upon fear memory retrieval (Li *et al*, 2013). Our findings add the notion that CeL neurons give

rise to a long-range axonal projection onto NPS neurons and that functional efficacy of this projection is enhanced upon fear memory retrieval. The reduction of failure rate and increased paired-pulse depression following fear memory retrieval would indicate a presynaptic site of plasticity, although further experiments are needed to precisely identify the locus and mechanisms of plasticity. Overall our findings suggest a mechanism, which strengthens the excitatory drive onto $fear_{on}$ neurons in the CeL (Li *et al*, 2013), and in addition, enhances the efficacy of output synapses on NPS neurons during retrieval of fear. Thereby, processing of fear signals seems to involve local amygdalar mechanisms within the CeL and at the same time remote synaptic mechanisms that boost CeL-mediated GABAergic inhibition of NPS neurons in the brainstem.

By using retrograde tracer and immunohistochemistry, we show that a subpopulation of CeL neurons with projections to the periLC/LC region is dynorphinergic (see also Reyes *et al*, 2008,2011). Moreover, the combination of behavioral experiments and immunohistochemistry for pCREB, a marker of neuronal activation (Hall *et al*, 2001; Izumi *et al*, 2011; Sargin *et al*, 2013), revealed that dynorphinergic neurons in the CeL are activated during fear memory retrieval as they displayed a significant increase in nuclear pCREB fluorescence intensity and abundance (Deisseroth *et al*, 1996; Hall *et al*, 2001; Han *et al*, 2007; Hsiang *et al*, 2014; Izumi *et al*, 2011). A similar increase of the expression of the immediate early gene *c-fos* was observed in SOM-positive CeL neurons of fear-conditioned mice (Li *et al*, 2013). Our data show that pdyn-positive CeL neurons are a subpopulation of the SOM-positive/PKCδ-negative neurons, and thus functionally represent $fear_{on}$ neurons. In line with this, pdyn- and SOM-positive fibers are present in the periLC region and electrophysiological recordings revealed that NPS neurons in the periLC are inhibited by dynA and SOM, which are acting via postsynaptic receptors to induce membrane hyperpolarization. Despite the possibility that also local dynorphinergic neurons might be present in the LC region and although direct evidence for a synaptic release of dynorphin or SOM from CeL fibers is lacking, it is tempting to speculate that dynorphin and SOM are coactive in fear-activated GABAergic projections from CeL to NPS neurons in the brainstem. If synaptically activated, these peptidergic systems could act in synergy with GABA to decrease activity of postsynaptic NPS target neurons (Figure 5e). Moreover, our data indicate that also projections from the CeM contribute to GABAergic transmission onto NPS neurons in the periLC region. Overall, fear-relevant CeL and CeM neurons are suited to inhibit parts of the NPS system during fear memory retrieval (Figure 5e).

A convergent line of evidence indicates that the activation of NPS system is augmented upon stress exposure. Stress in rodents activates NPS neurons in the LC/periLC region (Jungling *et al*, 2012; Liu *et al*, 2011), resulting in an increased release of NPS into the BA (Ebner *et al*, 2011), and application of NPS into the BA improves stress coping in a conditioned fear memory and extinction paradigm (Chauveau *et al*, 2012). In addition, NPS regulates synaptic interactions of neurons in the basal amygdala and of GABAergic intercalated cells (Jungling *et al*, 2008; Meis *et al*, 2008,2011), resulting in an overall anxiolytic-like effect, facilitation of fear extinction and buffering of stress-evoked increases of anxiety (Chauveau *et al*, 2012). An inhibitory modulation of the NPS system by dynorphin is of particular interest, given the anxiogenic-like action of dynorphin upon stressful encounters (for review see: Knoll and Carlezon, 2009). More specifically, dynorphin is released during stress exposure (McLaughlin *et al*, 2003), and mediates a variety of stress-related and -induced behaviors (Carey *et al*, 2009; Land *et al*, 2008; Mague *et al*, 2003; McLaughlin *et al*, 2003). Although dynorphin-containing fibers in the LC itself, which originate in central amygdalar sources have been described by neuroanatomical studies in great detail (Reyes *et al*, 2007, 2008, 2011), our work indicates that these fibers innervate also NPS neurons in the periLC. Recently, it was shown in mice that a subpopulation of fear-relevant SOM-neurons in the CeL project to the periaqueductal grey (PAG) and paraventricular thalamic nucleus (Penzo *et al*, 2014). This indicates that SOM-positive CeL neurons might, in concert with CeM neurons, drive fear expression via disinhibition of the ventral PAG (Penzo *et al*, 2014). There are evidences that activation of SOM-receptors 2 in LC neurons leads to inhibition and results in decreased spontaneous firing (Chessell *et al*, 1996). Similarly, in the lateral amygdala SOM exerts inhibitory action and influences contextual fear memory (Kluge *et al*, 2008; Meis *et al*, 2005). Our data suggest that SOM-/dynA-neurons from the CeL might innervate also NPS neurons in the periLC and employ inhibitory mechanisms to dampen neuronal excitability, although the release of these peptides from CeL terminals onto NPS neurons remains to be investigated.

According to the present findings activation of these CeL/CeM neurons, as for instance during fear memory retrieval, will inhibit NPS neurons and by this it will limit the release of NPS leading to states of heightened stress responsiveness and fear. Summarizing, the fear-relevant neurons in the CeL directly interfere with anxiolytic NPS system via long-range axonal projections, containing GABA and potentially coactive peptides, SOM, and dynorphin. This circuit seems paramount for the regulation of fear responses upon stressful encounters (Figure 5e), and any alteration in neurons within the loop between NPS neurons in the periLC and amygdala, such as polymorphisms of the mentioned peptides or their receptors might be an attractive target for stress and anxiety disorder research.

FUNDING AND DISCLOSURE

This project was funded by the German research foundation (grants: DFG; SFB-TR58, TPA03 to H-CP; DFG; SFB-TR58, TPA07 to KJ; and DFG; SFB, SFB-TR58, TPA02 to H-CP), the IZKF (Interdisciplinary Centre for Clinical Research, Münster; grant: PaHC3/003/10 to H-CP and KJ), and a Max Planck Research Award (to H-CP). The authors declare no conflict of interest.

ACKNOWLEDGMENTS

We thank Julia Schröer, Elke Naß, Petra Berenbrock, Birgit Herrenpoth, Angelika Klinge, and Svetlana Kiesling for excellent technical assistance. We thank Dr Philippe Coulon for critical reading of the manuscript. Transgenic NPS-EGFP mice were a kind gift of Professor Rainer Reinscheid (University of California, Irvine, CA, USA).

REFERENCES

Carey AN, Lyons AM, Shay CF, Dunton O, McLaughlin JP (2009). Endogenous kappa opioid activation mediates stress-induced deficits in learning and memory. *J Neurosci* **29**: 4293–4300.

Charney DS (2003). Neuroanatomical circuits modulating fear and anxiety behaviors. *Acta Psychiatr Scand Suppl* **108**: 38–50.

Chauveau F, Lange MD, Jungling K, Lesting J, Seidenbecher T, Pape HC (2012). Prevention of stress-impaired fear extinction through neuropeptide s action in the lateral amygdala. *Neuropsychopharmacology* **37**: 1588–1599.

Chessell IP, Black MD, Feniuk W, Humphrey PP (1996). Operational characteristics of somatostatin receptors mediating inhibitory actions on rat locus coeruleus neurones. *Br J Pharmacol* **117**: 1673–1678.

Ciocchi S, Herry C, Grenier F, Wolff SB, Letzkus JJ, Vlachos I *et al* (2010). Encoding of conditioned fear in central amygdala inhibitory circuits. *Nature* **468**: 277–282.

Deisseroth K, Bito H, Tsien RW (1996). Signaling from synapse to nucleus: postsynaptic CREB phosphorylation during multiple forms of hippocampal synaptic plasticity. *Neuron* **16**: 89–101.

Dimitrov EL, Yanagawa Y, Usdin TB (2013). Forebrain GABAergic projections to locus coeruleus in mouse. *J Comp Neurol* **521**: 2373–2397.

Donner J, Haapakoski R, Ezer S, Melen E, Pirkola S, Gratacos M *et al* (2010). Assessment of the neuropeptide S system in anxiety disorders. *Biol Psychiatry* **68**: 474–483.

Douglass J, McKinzie AA, Pollock KM (1994). Identification of multiple DNA elements regulating basal and protein kinase A-induced transcriptional expression of the rat prodynorphin gene. *Mol Endocrinol* **8**: 333–344.

Ebner K, Rjabokon A, Pape HC, Singewald N (2011). Increased *in vivo* release of neuropeptide S in the amygdala of freely moving rats after local depolarisation and emotional stress. *Amino Acids* **41**: 991–996.

Fanselow MS (1980). Conditioned and unconditional components of post-shock freezing. *Pavlov J Biol Sci* **15**: 177–182.

Hall J, Thomas KL, Everitt BJ (2001). Fear memory retrieval induces CREB phosphorylation and Fos expression within the amygdala. *Eur J Neurosci* **13**: 1453–1458.

Han JH, Kushner SA, Yiu AP, Cole CJ, Matynia A, Brown RA *et al* (2007). Neuronal competition and selection during memory formation. *Science* **316**: 457–460.

Haubensak W, Kunwar PS, Cai H, Ciocchi S, Wall NR, Ponnusamy R *et al* (2010). Genetic dissection of an amygdala microcircuit that gates conditioned fear. *Nature* **468**: 270–276.

Hsiang HL, Epp JR, van den Oever MC, Yan C, Rashid AJ, Insel N *et al* (2014). Manipulating a "cocaine engram" in mice. *J Neurosci* **34**: 14115–14127.

Itoi K, Sugimoto N (2010). The brainstem noradrenergic systems in stress, anxiety and depression. *J Neuroendocrinol* **22**: 355–361.

Izumi T, Boku S, Shinmin W, Inoue T, Konno K, Yamaguchi T *et al* (2011). Retrieval of conditioned fear activates the basolateral and intercalated nucleus of amygdala. *J Neurosci Res* **89**: 773–790.

Jungling K, Liu X, Lesting J, Coulon P, Sosulina L, Reinscheid RK *et al* (2012). Activation of neuropeptide S-expressing neurons in the locus coeruleus by corticotropin-releasing factor. *J Physiol* **590**: 3701–3717.

Jungling K, Seidenbecher T, Sosulina L, Lesting J, Sangha S, Clark SD *et al* (2008). Neuropeptide S-mediated control of fear expression and extinction: role of intercalated GABAergic neurons in the amygdala. *Neuron* **59**: 298–310.

Kluge C, Stoppel C, Szinyei C, Stork O, Pape HC (2008). Role of the somatostatin system in contextual fear memory and hippocampal synaptic plasticity. *Learn Mem* **15**: 252–260.

Knoll AT, Carlezon WA Jr. (2009). Dynorphin, stress, and depression. *Brain Res* **1314**: 56–73.

Land BB, Bruchas MR, Lemos JC, Xu M, Melief EJ, Chavkin C (2008). The dysphoric component of stress is encoded by activation of the dynorphin kappa-opioid system. *J Neurosci* **28**: 407–414.

Laxmi TR, Stork O, Pape HC (2003). Generalisation of conditioned fear and its behavioural expression in mice. *Behav Brain Res* **145**: 89–98.

Li H, Penzo MA, Taniguchi H, Kopec CD, Huang ZJ, Li B (2013). Experience-dependent modification of a central amygdala fear circuit. *Nat Neurosci* **16**: 332–339.

Liu X, Zeng J, Zhou A, Theodorsson E, Fahrenkrug J, Reinscheid RK (2011). Molecular fingerprint of neuropeptide S-producing neurons in the mouse brain. *J Comp Neurol* **519**: 1847–1866.

Mague SD, Pliakas AM, Todtenkopf MS, Tomasiewicz HC, Zhang Y, Stevens WC Jr. *et al* (2003). Antidepressant-like effects of kappa-opioid receptor antagonists in the forced swim test in rats. *J Pharmacol Exp Ther* **305**: 323–330.

McLaughlin JP, Marton-Popovici M, Chavkin C (2003). Kappa opioid receptor antagonism and prodynorphin gene disruption block stress-induced behavioral responses. *J Neurosci* **23**: 5674–5683.

Meis S, Bergado-Acosta JR, Yanagawa Y, Obata K, Stork O, Munsch T (2008). Identification of a neuropeptide S responsive circuitry shaping amygdala activity via the endopiriform nucleus. *PLoS One* **3**: e2695.

Meis S, Sosulina L, Schulz S, Hollt V, Pape HC (2005). Mechanisms of somatostatin-evoked responses in neurons of the rat lateral amygdala. *Eur J Neurosci* **21**: 755–762.

Meis S, Stork O, Munsch T (2011). Neuropeptide S-mediated facilitation of synaptic transmission enforces subthreshold theta oscillations within the lateral amygdala. *PLoS One* **6**: e18020.

Okamura N, Garau C, Duangdao DM, Clark SD, Jungling K, Pape HC *et al* (2011). Neuropeptide S enhances memory during the consolidation phase and interacts with noradrenergic systems in the brain. *Neuropsychopharmacology* **36**: 744–752.

Pare D, Quirk GJ, Ledoux JE (2004). New vistas on amygdala networks in conditioned fear. *J Neurophysiol* **92**: 1–9.

Penzo MA, Robert V, Li B (2014). Fear conditioning potentiates synaptic transmission onto long-range projection neurons in the lateral subdivision of central amygdala. *J Neurosci* **34**: 2432–2437.

Petrella C, Agostini S, Guerrini R, Calo G, Giaquinto A, De Nuccio C *et al* (2011). Neuropeptide S inhibits stress-stimulated faecal output in the rat. *Pharmacol Res* **64**: 471–477.

Petrovich GD, Canteras NS, Swanson LW (2001). Combinatorial amygdalar inputs to hippocampal domains and hypothalamic behavior systems. *Brain Res Brain Res Rev* **38**: 247–289.

Reinscheid RK (2008). Neuropeptide S: anatomy, pharmacology, genetics and physiological functions. *Results Probl Cell Differ* **46**: 145–158.

Reinscheid RK, Xu YL, Civelli O (2005). Neuropeptide S: a new player in the modulation of arousal and anxiety. *Mol Interv* **5**: 42–46.

Reyes BA, Carvalho AF, Vakharia K, Van Bockstaele EJ (2011). Amygdalar peptidergic circuits regulating noradrenergic locus coeruleus neurons: linking limbic and arousal centers. *Exp Neurol* **230**: 96–105.

Reyes BA, Drolet G, Van Bockstaele EJ (2008). Dynorphin and stress-related peptides in rat locus coeruleus: contribution of amygdalar efferents. *J Comp Neurol* **508**: 663–675.

Reyes BA, Johnson AD, Glaser JD, Commons KG, Van Bockstaele EJ (2007). Dynorphin-containing axons directly innervate noradrenergic neurons in the rat nucleus locus coeruleus. *Neuroscience* **145**: 1077–1086.

Sangha S, Ilenseer J, Sosulina L, Lesting J, Pape HC (2012). Differential regulation of glutamic acid decarboxylase gene expression after extinction of a recent memory vs. intermediate memory. *Learn Mem* **19**: 194–200.

Sara SJ (2009). The locus coeruleus and noradrenergic modulation of cognition. *Nat Rev Neurosci* **10**: 211–223.

Sargin D, Mercaldo V, Yiu AP, Higgs G, Han JH, Frankland PW *et al* (2013). CREB regulates spine density of lateral amygdala neurons: implications for memory allocation. *Front Behav Neurosci* **7**: 209.

Seidenbecher T, Laxmi TR, Stork O, Pape HC (2003). Amygdalar and hippocampal theta rhythm synchronization during fear memory retrieval. *Science* **301**: 846–850.

Tye KM, Prakash R, Kim SY, Fenno LE, Grosenick L, Zarabi H *et al* (2011). Amygdala circuitry mediating reversible and bidirectional control of anxiety. *Nature* **471**: 358–362.

Viviani D, Charlet A, van den Burg E, Robinet C, Hurni N, Abatis M *et al* (2011). Oxytocin selectively gates fear responses through distinct outputs from the central amygdala. *Science* **333**: 104–107.

Xu YL, Reinscheid RK, Huitron-Resendiz S, Clark SD, Wang Z, Lin SH *et al* (2004). Neuropeptide S: a neuropeptide promoting arousal and anxiolytic-like effects. *Neuron* **43**: 487–497.

Supplementary Information accompanies the paper on the Neuropsychopharmacology website (http://www.nature.com/npp)